AUTHOR(S): WANG, S., FERNANDEZ, C., SHANG, L., LI, Z. and YUAN, H.

TITLE: An integrated online adaptive state of charge estimation approach of high-power lithium-ion battery packs.

YEAR: 2018

Publisher citation: WANG, S., FERNANDEZ, C., SHANG, L., LI, Z. and YUAN, H. 2018. An integrated online adaptive state of charge estimation approach of high-power lithium-ion battery packs. Transactions of the Institute of Measurement and Control [online], 40(6), pages 1892-1910. Available from: https://doi.org/10.1177/0142331217694681

OpenAIR citation: WANG, S., FERNANDEZ, C., SHANG, L., LI, Z. and YUAN, H. 2018. An integrated online adaptive state of charge estimation approach of high-power lithium-ion battery packs. Transactions of the Institute of Measurement and Control, 40(6), pages 1892-1910. Held on OpenAIR [online]. Available from: https://openair.rgu.ac.uk

Article

TRANSACTIONS OF THE INSTITUTE OF MEASUREMENT & CONTROL

Transactions of the Institute of Measurement and Control
1–19

DOI: 10.1177/0142331217694681
journals.sagepub.com/home/tim
SAGE

An integrated online adaptive state of charge estimation approach of high-power lithium-ion battery packs

Shunli Wang[1], Carlos Fernandez[2], Liping Shang[1], Zhanfeng Li[3] and Huifang Yuan[4]

Abstract

A novel online adaptive state of charge (SOC) estimation method is proposed, aiming to characterize the capacity state of all the connected cells in lithium-ion battery (LIB) packs. This method is realized using the extended Kalman filter (EKF) combined with Ampere-hour (Ah) integration and open circuit voltage (OCV) methods, in which the time-scale implementation is designed to reduce the computational cost and accommodate uncertain or time-varying parameters. The working principle of power LIBs and their basic characteristics are analysed by using the combined equivalent circuit model (ECM), which takes the discharging current rates and temperature as the core impacts, to realize the estimation. The original estimation value is initialized by using the Ah integral method, and then corrected by measuring the cell voltage to obtain the optimal estimation effect. Experiments under dynamic current conditions are performed to verify the accuracy and the real-time performance of this proposed method, the analysed result of which indicates that its good performance is in line with the estimation accuracy and real-time requirement of high-power LIB packs. The proposed multi-model SOC estimation method may be used in the real-time monitoring of the high-power LIB pack dynamic applications for working state measurement and control.

Keywords

Equivalent circuit model, extended Kalman filter, lithium-ion battery, online estimation, state of charge

Introduction

In recent years, lithium-ion battery (LIB) packs have attracted particular attention in power supply applications for their high power density, high energy density, low self-discharge rate, long cycle life and longevity advantages, and have gained in popularity as the energy source for many applications, ranging from portable equipment, electric vehicles (EVs) and renewable energy systems to airborne equipment and other applications. LIB packs are used in the discharging and charging maintenance (DCM) processes in order to supply energy reliably, in which the battery cell voltage, total voltage, temperature and other parameters should be detected in real time to prolong the service life and cycling number of the LIB packs. In recent years, with continuous improvement in the science and technology of materials, production technology and other aspects, the performance of LIB packs continues to improve with reduced cost and it has gradually become the most promising rechargeable battery. LIB packs, because of their lightweight, high energy density, high rate discharge performance, no pollution to the environment and other advantages, have started to be used in hybrid electric buses, EVs, underwater weapons, water navigation, aerospace and other fields. However, the safety of high-power LIB packs is still the most concerning problem. Improper LIB energy management will directly affect its energy supply efficiency and useful life, in which severe cases may also lead to security incidents. Therefore, the state of charge (SOC) estimation for an LIB pack in its entire life cycle is necessary, through which the remaining useful energy of an LIB pack may be known in real time. According to the working status monitoring of the LIB pack in its DCM process, the overall performance of the LIB pack may be given an accurate evaluation.

Due to the high power and energy requirements, a LIB is usually used in series and parallel conditions with mounts of battery cells. Battery security protection is becoming the main challenge because of of accidents caused by uncontrolled

[1]School of Information Engineering & Robot Technology Used for Special Environment Key Laboratory of Sichuan Province, Southwest University of Science and Technology, Mianyang, Sichuan, China
[2]School of Pharmacy and Life Sciences, Robert Gordon University, Aberdeen, UK
[3]School of Manufacturing Science and Engineering, Southwest University of Science and Technology, Mianyang, Sichuan, China
[4]School of Economics and Management, Southwest University of Science and Technology, Mianyang, Sichuan, China

Corresponding author:
Shunli Wang, School of Information Engineering & Robot Technology Used for Special Environment Key Laboratory of Sichuan Province, Southwest University of Science and Technology, 59 Middle Qinglong Road Fucheng District, Mianyang 621010 P.R. China, Mianyang, Sichuan 621010, China.
Email: wangshunli@swust.edu.cn

Table 1. List of symbols used in the paper.

Symbol	Full-name	Description
Ah	Ampere-hour	The SOC value is obtained by the method of current and time integration
BMS	Battery management system	An apparatus for energy management of the lithium ion battery pack
BMTS	Battery maintenance and testing system	The device for the ground maintenance and testing of the battery pack
CC	Constant current	The constant current mode for charging or discharging
CV	Constant voltage	The constant voltage mode for charging or discharging
DCM	Discharging and charging maintenance	Maintenance process of charging and discharging
ECM	Equivalent circuit model	Battery performance simulation based on equivalent circuit
EKF	Extended Kalman filter	KF-based estimation method using Taylor series expansion
IR	Internal resistance	The internal resistance of the lithium ion battery
KF	Kalman filter	A state estimation method using Kalman filter
LIB	Lithium ion battery	Lithium ion battery with lithium cobalt acid type
MMSE	Minimum mean square error	Method for evaluating the effect of an estimation
NN	Neural network	The SOC estimation method by simulating human nerve
OCV	Open circuit voltage	Battery voltage after long standing
RMSE	Root mean square error	A method for evaluating detection error
SOC	State of charge	A parameter to characterize the remaining battery power
UKF	Unscented Kalman filter	A KF-based estimation method using the unscented transformation

working states of the LIB packs. Industrial applications of the LIB packs usually require well-designed management systems to protect safety and make them show good working performance, and monitor the running status in real time and control its power supply process. The associated battery management system (BMS) equipment is usually used to facilitate the safety and efficiency of the LIB packs and the SOC value is an important aspect, the inaccurate estimation of which will make the BMS equipment hardly provide sufficient energy management and affect the safety of the battery power supply system (Saw, 2016; Su, 2016; Tabuchi, 2016; Yang, 2016; Ye, 2016; Yu, 2016; Zhu, 2016). To safeguard the safety and working performance of an LIB pack, reliable and accurate SOC estimation is required in the associated BMS equipment of the LIB pack. The dynamic models derived either from equivalent circuits or electrochemical principles facilitate the assimilation of the battery data and lead to an SOC estimation value with bounded errors.

Many methods may used to estimate the SOC value for LIBs, such as the Ampere-hour (Ah) integration and open circuit voltage (OCV) methods, which are studied by Arbabzadeh et al.(2016), Burgos-Mellado et al.(2016) and Gallien et al.(2015). Dynamic and closed-loop model-based methods such as the extended Kalman filter (EKF), neural network (NN), fuzzy logic and equivalent circuit model (ECM) have been extensively used in SOC estimation (Beattie, 2016; Dong, 2016; Masoumnezhad, 2015; Ganesan, 2016; Mohammad,2016; Tenfen,2016). Several solutions to this issue have been reported in recent years and each has its relative merits. In particular, the SOC estimation tests of LIBs have been widely studied using the Kalman filter (KF) methods, which have been remarkable in this aspect. Aung et al. (2015) proposed a square-root spherical unscented Kalman filter (UKF) method for the SOC estimation for the LIB used in a nano-satellite. The SOC estimation methods based on the flexible transformation of the KF algorithm are widely used and have made significant achievements in different applications, such as classical linear KF, EKF, UKF and iterated EKF, and so on. A relatively complete battery model is the prerequisite of the SOC estimation realization, along with the dynamic modelling and parameter identification. However, it is difficult to obtain an accurate online model because it is subject to the changes of time and working conditions (Cao, 2016; Fabri, 2015; Fridholm, 2016; Ge, 2016; Mohammad, 2016). Furthermore, the internal resistance (IR) value of the LIB will increase along with time, and the capacity diminishes as a result of the degradation. Because the battery cell may differ from one cell to another, this makes parameter identification of each cell is rather cumbersome; thus it is desirable to use the adaptive models, in which the parameter identification and SOC estimation process is just merged into a single one-model construction. The symbols used in the paper are described in Table 1.

A real-time joint estimator is constructed by Gao et al. (2015) for the model parameters and the SOC determination of LIBs in EVs. A novel Gaussian model based on battery state estimation approach was proposed by He et al. (2015) and named SOE. Two-time-scaled battery model identification was studied by Hu et al. (2015) with application to battery state estimation. Capacity fade estimation was done by Hussein (2015) for LIBs in EVs using the artificial neural network (ANN) algorithm. Fading KF-based real-time SOC estimation was conducted by Lim et al. (2016) in LIB-powered EVs. An LIB pack capacity estimation approach was proposed by Wang LM et al. (2015), considering in-parallel cell safety in EVs. On-board SOH estimation was conducted by Wang SL et al. (2015) at a wide ambient temperature range in LIBs. Probability-based remaining capacity estimation was conducted by Wang QS et al. (2016) using data-driven and NN models.

Mounts of LIB cells are used as series or parallel in the power LIB pack, which is aiming to meet the high energy and voltage requirements of the power supply systems. Due to the restrictions of material defects, contamination and production technology tolerances, there are dynamic and aging characteristic differences among the connected LIB cells (Burow, 2016; Ciez, 2016; Elsayed, 2016; Jaguemont, 2016; Jia, 2015). The information parameters of working conditions, temperature distributions, IR difference and historical state also influence the SOC value of the LIB packs. The SOC value of each

individual cell should be also estimated by the associated BMS equipment for reliable and accurate power supply management. An effective solution is that the adaptive SOC estimator should be designed to calculate the SOC value of each single cell, considering the above parameters, and replicated for all connected cells in the LIB pack, which will obviously incur a high computational cost and is not suitable for online implementation in an embedded system.

A novel LIB balancing strategy was proposed by Shang et al. (2014) based on a global best-first and integrated imbalance calculation. Adaptive non-linear model-based fault diagnosis was conducted by Sidhu et al. (2015) for LIBs. The optimization method was proposed by Song et al. (2015) for a hybrid energy storage system in EVs using a dynamic programming approach. The online dynamic equalization adjustment method was studied by Wang SL et al. (2016) for high-power LIB packs based on the SOB estimation. The controllability is evaluated by Zhai et al. (2014) for a class of switching control systems and application to the kinetic battery model.

Mounts of SOC estimation methods have been proposed, each method of which has its own advantages and limitations. Generally, these methods may be mainly classified into two kinds: direct measurement-based estimation and model-based estimation. The first method directly uses the measurements from the battery system to calculate the SOC, such as Ah and OCV-based methods. The Ah algorithm is easy to implement with low computational cost, but it suffers from low estimation accuracy due to the accumulative errors caused by the current sensor noise and it is difficult to obtain the initial SOC. Therefore, the OCV method is usually used to complement the Ah method to recalibrate the SOC and provide the initial SOC. However, a long rest time of the tested battery is required to reach the OCV, which is usually unrealistic for the actual applications. In the second kind of method, the battery model is utilized when estimating the battery SOC. One of the model-based methods for SOC estimation is based on the black box battery models, such as NNs, fuzzy logic and support vector machine, which may be quite accurate if sufficient experimental data is used to train the model. However, their performance greatly depends on the quantity and quality of the training data set, and a large amount of offline battery tests are necessary to obtain a good model, which may be very time-consuming. The optimum state filtering method is another kind of model-based method for battery SOC estimation. This method usually performs SOC estimation based on the ECM, such as EKF, sigma point KF, adaptive EKF, adaptive UKF and so on.

As the EKF suffers from the drawbacks of the Jacobian matrix derivation and linearization accuracy, the adaptive estimation model is developed by using the EKF algorithm, combined with the ECM, OCV and Ah integral methods. The method is validated experimentally by the measurement results of the LIBs with little computational requirement. Due to the rigorous requirements on real time and sampling synchronization, the battery maintenance and testing system (BMTS) based on RS485 and PCI is also designed for the implementation of this method. In order to realize the adaptive, high accuracy and easy implement SOC estimation, the combined model was proposed and realized, the estimation characteristics of which are analysed in this study. The proposed method has been validated with experimental results and benchmarked with an integrated circuit and the Coulomb counting methods. The results have been shown that the proposed method has a lower absolute mean, absolute minimum mean square error (MMSE) and root mean square error (RMSE) than the single OCV, Ah integration or EKF methods (Wijewardana, 2016; Tong, 2015; Schindler, 2016; Samadani, 2016; Raisemche, 2016). The experimental results showed the clearness of the proposed method for reliable SOC estimation.

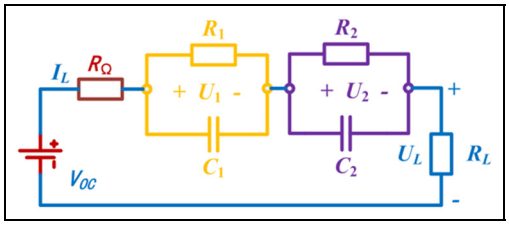

Figure 1. The second-order resistor–capacitor (RC) battery model.

The rest of the paper is organized as follows. In the next section, we present a basic principle of EKF and its improvement for SOC estimation. Then we describe the model construction process, and the battery state and measurement equations based on the battery impact factor analysis. Its effective characteristics are validated by the simulation and experiment results shown. Finally, conclusions and future work ideas are discussed.

The associated model for the SOC estimation

Compared with other battery models, the ECM may show the relationship between the input current and the output voltage more intuitively, which benefits the identification of cell characterization and model parameters. Therefore, the battery ECM is built for SOC estimation, the establishment process of which contains two aspects of accuracy and complexity as the main factors. It is necessary to reflect the dynamic characteristics of the battery for the engineering applications.

Battery ECM structure construction

The battery charging and discharging maintenance process is performed, during which the terminal voltage response after the end of the charge and discharge is fitted by one, two and three orders. The higher the order of the ECM, the closer the data fits to the actual experiment data. However, the higher the order for the model, the higher the degree of model complexity. When the model is used for the SOC online estimations of the power supply LIB pack, a longer calculation time is needed, as a greater amount of calculation is used (Kim, 2016; Klein, 2016; Li Y, 2016; Lu, 2016; Panchal, 2016; Pramanik, 2016; Rahman, 2016). The error of the second-order fitting process is much smaller than the first-fitting process, but it is almost the same as the third-order fitting error. As a result, the second-order resistor–capacitor (RC) ECM is

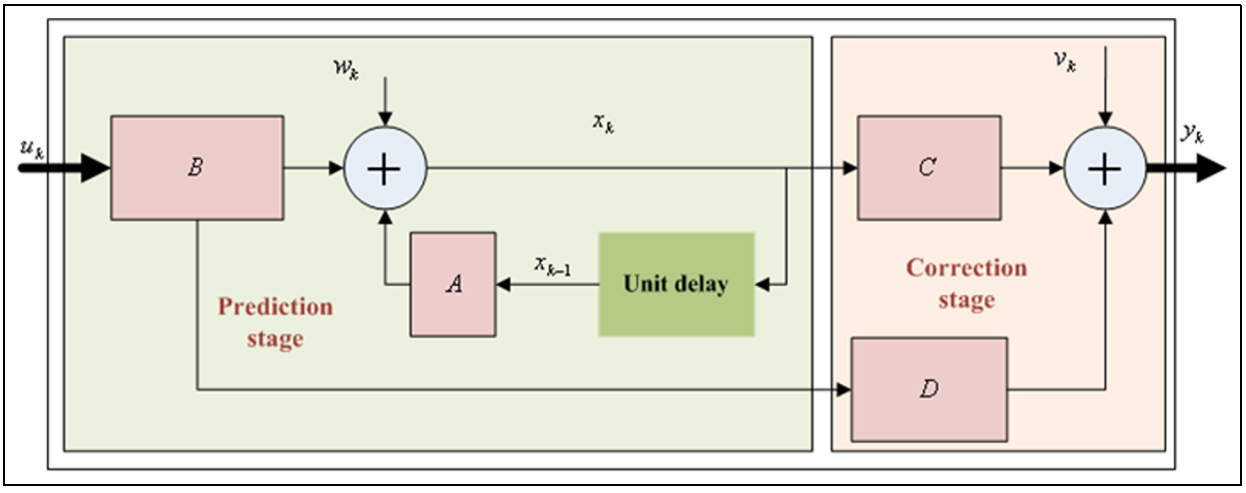

Figure 2. The state-space model structure of the extended Kalman filter (EKF) algorithm.

used for the SOC estimation, shown in Figure 1, in which V_{OC} indicates the OCV value of LIB, which has non-linear relationship with SOC; R_0 represents the resistance of active material, collectors, conductive tabs, the fluid collector and the contact resistance among them; R_1 and C_1 denote the diffusion layer resistance and capacitance, respectively; R_2 and C_2 are the resistors and capacitors of the close layer; I expresses the charging or discharging current, the value of which is negative when charged and positive when discharged; and V is the cell terminal voltage.

The ECM has one more RC circuit than the ECM used by Lee et al. (2015) and has better performance for the LIB characterization.

According to the second-order RC battery model shown in Figure 1, the state-space model is obtained as shown in Equations (1) and (2). It is combined with the Ah integration method to realize the SOC estimation, in which the terminal voltages of V_1 and V_2 at the ends of the capacitors of C_1 and C_2 are used as the state variables. Φ is used to characterize the battery SOC. The charging or discharging current parameter I is used as the input variable and the battery terminal voltage parameter V is used as the output variable.

$$\begin{bmatrix} V_1(k+1) \\ V_2(k+1) \\ \Phi(k+1) \end{bmatrix} = \begin{bmatrix} R_1\left(1-\exp\left(-\frac{\Delta t}{R_1C_1}\right)\right) \\ R_2\left(1-\exp\left(-\frac{\Delta t}{R_2C_2}\right)\right) \\ -\frac{\eta\Delta t}{C_N} \end{bmatrix} I(k) + \begin{bmatrix} \exp\left(-\frac{\Delta t}{R_1C_1}\right) & 0 & 0 \\ 0 & -\frac{\Delta t}{R_2C_2} & 0 \\ 0 & 0 & 1 \end{bmatrix} \begin{bmatrix} V_1(k) \\ V_2(k) \\ \Phi(k) \end{bmatrix} \quad (1)$$

$$V(k) = \begin{bmatrix} -1 & -1 & \frac{dV_{OC}(\Phi)}{d\Phi} \end{bmatrix} \begin{bmatrix} V_1(k) \\ V_2(k) \\ \Phi(k) \end{bmatrix} - R_0 I(k) \quad (2)$$

The battery SOC is estimated by using the adaptive EKF method based on this space model. The parameters in the space model shown in Equations (1) and (2) are described as follows: Δt is the sampling interval, the value of which is initialized as $\Delta t = 1$ s. The sampling interval time parameter has no influence on the SOC estimation results in the simulation process, but it will affect the application of the BMS equipment in the power LIB pack. The large sampling interval value will increase in the cumulative estimation error, and the small sampling interval value will increase the computational burden of the processor. Considering the online SOC estimation demand, a value of 1 s is selected in the actual BMS application. In order to match this, a value of 1 s is also selected as the sampling interval time in the simulation process. $V_1(k)$, $V_2(k)$ and $\Phi(k)$ denote the kth sampling Φ value and the voltage across the capacitor of C_1 and C_2; $V_1(k+1)$, $V_2(k+1)$ and $\Phi(k+1)$ denote the voltage and Φ value, respectively, at the $k+1$ sampling time. η is the Coulomb efficiency and C_N indicates the battery total capacity calculated by Ah integration method; V_{OC} indicate the open-circuit voltage, which is a function of Φ. They have the same order as the ECM used by Perez et al. (2015), and are integrated in the closed-loop algorithm and able to compensate for them to correct the SOC value.

Combined estimation based on EKF

In terms of the battery SOC estimation methods, many research approaches have previously been proposed. Due to the closed-loop estimation ability and strong inhibiting effect on noise, the KF-based SOC estimator has been widely studied. The KF algorithm was proposed by Kalman and its application range is only suitable for linear equations and linear systems. When it comes to non-linear recursive equations, it is necessary to use the linearization treatment to estimate the model parameters, such as the EKF, UKF, IEKF algorithms and so on.

EKF algorithm for estimation. The EKF algorithm is a state-space model that is based on the dynamic liner state equations and the linearization treatment of the non-linear characteristics of the OCV towards SOC. The structure of the EKF algorithm is shown in Figure 2.

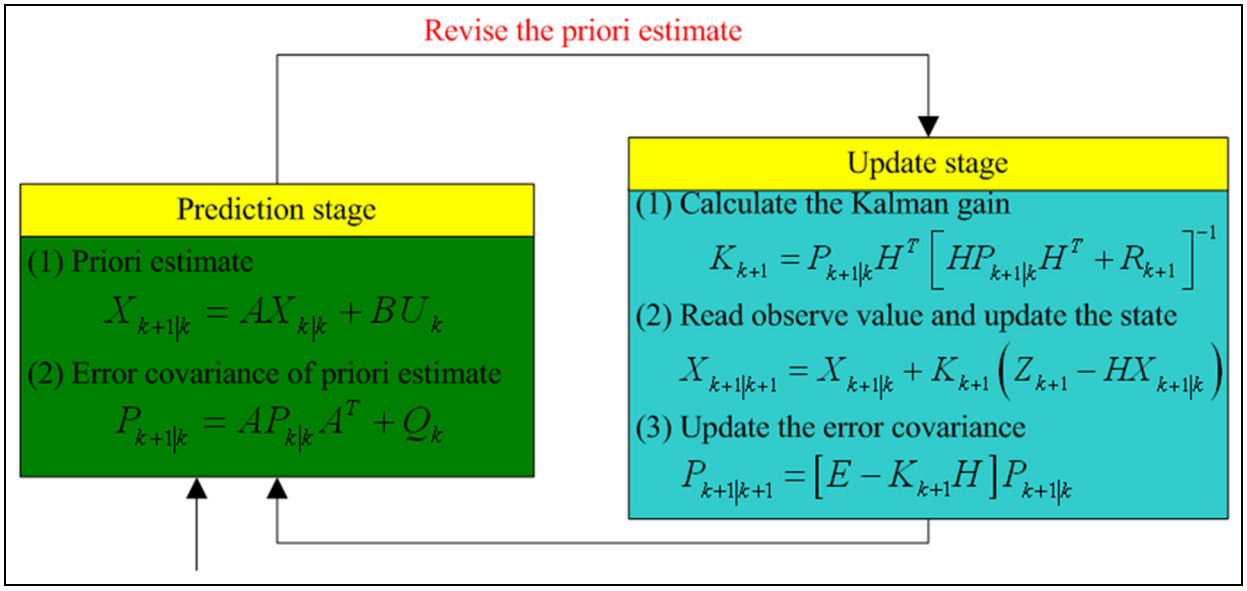

Figure 3. The recursive process principle of the extended Kalman filter (EKF) algorithm.

The state-space model, including the state equation and the observation equation, is thus

$$\begin{cases} X_{k+1} = AX_k + BU_k + W_k \\ Z_{k+1} = HX_{k+1} + V_{k+1} \end{cases} \tag{3}$$

where the first part of the function is the system state equation and the second part is the measurement function; k is the dispersive time interval; X_k is the system state factor at time point k; Z_k is the state measurement factor at time point k; U_k is the control signal at time point k; W_k is the input noise at time point k; and V_k is the measurement noise at time point k, the parameter ranges of which are in the scope of $W_k \sim (0, Q_k)$ and the range of $V_k \sim (0, R_k)$. The recursive processing principle of the EKF algorithm is shown in Figure 3, in which $X_{k+1|k}$ indicates the prior estimation from the time point k state to the $k+1$ time state, namely the prediction value. $X_{k+1|k+1}$ indicates the posterior estimation from the time point k to the time point $k+1$, namely the optimal estimation value. The estimation process obtains the mean and covariance of the output of a non-linear function using a small fixed number of function evaluations.

Most battery state detection and control systems that we have encountered are non-linear systems. For example, the voltage output characteristics of the lithium iron phosphate battery show severe non-linearity. These systems cannot be analysed directly using the KF method, but need linearization treatments. However, the system state equation and system measurement equation of the LIB characteristics may be explored by using the Taylor series near the optimal estimation point. Then, the non-linear system may be translated into the linear system by dropping the high-order components, after treatment of which the experimental data may be handled by using the KF algorithm; this combined treatment at this time is named EKF. The linear process of the state equation and the measurement equation (observation equation) is analysed as follows. The state equation and measurement equation for the non-linear discrete state-space system may be simplified and expressed as shown:

$$\begin{cases} x_{k+1} = f(x_k, u_k) + \omega_k \\ y_k = g(x_k, u_k) + \nu_k \end{cases} \tag{4}$$

where the functions of $f(*)$ and $g(*)$ are non-liner equations. The upper equation in Equation (4) is the state equation, in which x is the n-dimensional system state vector and ω is an n-dimensional system noise vector at the time point k. The function $f(x_k,u_k)$ is the non-linear state transition function. The lower equation in Equation (4) is the observation equation, in which y is the m-dimensional system measurement vector and v is the m-dimensional system disturbance vector at time point k. The function $g(x_k,u_k)$ is the non-linear measurement function. The above functions may be explored by using Tailor method at the prior estimation point $x_{k+1|k}$ that is at the state x_{k+1}. The high-order components of the treatment process may be ignored and the liner approximations of $f(*)$ and $g(*)$ may be obtained as shown:

$$\begin{cases} f(x_k, u_k) \approx f\left(\hat{x}_{k|k-1}, u_k\right) + \left.\dfrac{\partial f(x_k, u_k)}{\partial x_k}\right|_{x_k = \hat{x}_{k|k-1}} \left(x_k - \hat{x}_{k|k-1}\right) \\ g(x_k, u_k) \approx g\left(\hat{x}_{k|k-1}, u_k\right) + \left.\dfrac{\partial g(x_k, u_k)}{\partial x_k}\right|_{x_k = \hat{x}_{k|k-1}} \left(x_k - \hat{x}_{k|k-1}\right) \end{cases} \tag{5}$$

The coefficients may be characterized by using the variables of M and H. Then, the liner state-space model may be obtained by lining from the non-liner system:

$$\begin{cases} x_{k+1} = M_k x_k + \left[f\left(\hat{x}_{k|k-1}, u_k\right) - M_k \hat{x}_{k|k-1}\right] + \omega_k, M_k \\ \quad = \left.\dfrac{\partial f(x_k, u_k)}{\partial x_k}\right|_{x_k = \hat{x}_{k|k-1}} \\ y_k = H_k x_k + \left[g\left(\hat{x}_{k|k-1}, u_k\right) - H_k \hat{x}_{k|k-1}\right] + \nu_k, H_k \\ \quad = \left.\dfrac{\partial g(x_k, u_k)}{\partial x_k}\right|_{x_k = \hat{x}_{k|k-1}} \end{cases} \tag{6}$$

M_k and H_k may be obtained by the above analysis, which may be used in the SOC state estimation and output voltage traction. The working state estimation characteristics may be gained from the above analysis, in which the advantages of this EKF-based SOC estimation method are shown as follows.

1) The recursive algorithm used in this method is quite suitable for the software programming, and it does not need to store a large amount of measured data, bringing out a very good real-time response performance.
2) The linearization treatment process may ameliorate the estimation error due to the measurement error of current, voltage, temperature, etc.
3) The state-space equation and the observation equation may ameliorate the measurement error caused by electromagnetic interference.
4) The effect of voltage rebound may be overcome by using updating process, which is suitable for the braking energy and the downhill potential energy recovery. The state estimation at any time of the application process for the LIB has a good effect.
5) The requirement of the initial state value is not high in the estimation process and the prediction may be tracked quickly in the real-time estimation process, which overcomes the shortcomings of other methods in the state estimation.

The function $E(x)$ indicates the expectation of the factor x and the function $Var(x)$ is its variance. $x_{k|k}$ is the measurement update of x; $x_{k|k-1}$ is the time update of x from the time point $k-1$ to the time point k. $P_{k|k}$ indicates the measurement error covariance update at time point k; $P_{k|k-1}$ is the time update of the error covariance from the time point $k-1$ to the time point k; Q_k is used as the system noise covariance matrix; R_k is used for the observation noise covariance matrix; and I is the identity matrix. The recursive filtering process of the system is shown as follows.

1) The initial condition of the filter equation is:

$$x_{0|0} = E(x), P_{0|0} = Var(x) \tag{7}$$

2) The update status of the estimation time is:

$$x_{k|k-1} = f(\hat{x}_k, u_k) \tag{8}$$

3) The time update of the error covariance is:

$$P_{k|k-1} = A_{k-1}P_{k-1|k-1}A^T{}_{k-1} + Q_{k-1} \tag{9}$$

4) The update process of Kalman gain matrix is:

$$K_k = P_{k|k-1}C_k^T\left(C_kP_{k|k-1}C_k^T + R_k\right)^{-1} \tag{10}$$

5) The measurement update of the estimation state is:

$$x_{k|k} = x_{k|k-1} + K_k[Y_k - g(\hat{x}_k, u_k)] \tag{11}$$

6) The measurement update of the error covariance is:

$$P_{k|k} = [I - K_kC_k]P_{k|k-1} \tag{12}$$

As seen from the recursive process of the EKF algorithm, the evaluation value of the system state is obtained by the addition of two parts, as shown in Equation (11). The first part is the time update of the estimation state, which indicates the present state estimation value that is obtained and updated by considering the last time moment system state and the latest input parameters. The second part is the detection amendment of the estimation state, which may revise the system state value by calculating the system error of the observation parameter and its estimation value, considering the Kalman gain parameter K_k.

Combined model of OCV and ECM. When the observed function is very accurate, the reserve amend value of the EKF filtering process may reduce the time update error, which makes the state estimation value quite close to the reference value. However, when the observe function is not accurate, the detection amendment may be not correct, which might even make the error between the detection update value of the estimation state and the reference value larger than the error between the time update value and the reference value.

A major drawback in the use of LIB arises from the strongly non-linear dependence and in wide ranges the flat characteristics of the battery OCV and the SOC. In addition, the hysteresis phenomenon has a distinct influence on the OCV. Then, the relationship of the battery OCV and SOC as well as the lack of dynamic models for LIBs hampers the determination of the SOC using state estimation techniques, resulting in high computational efforts to achieve an acceptable level of accuracy. Hence, it is desirable to measure a different physical parameter that varies more readily as a function of the SOC. To deal with the battery non-linear characteristics, the combined estimation method was proposed to build the battery SOC estimator.

The dynamic Kalman gain amend coefficient factor C is introduced into the estimation, which is multiplied by the Kalman gain matrix K. As a result, the weights of the time update of the estimation state and the detection amend value are determined. According to this process, the estimation value of SOC mainly depends on the time update process. However, when the observation function has high accuracy, the weight of the detection amend value may initially be a much larger value, which makes the estimation value of SOC mainly depend on the observed update process and obtains a higher convergence rate of the estimation value close to the reference value.

The combined ECM battery model is built and applied in the estimation process, which may make the state vector x of the EKF model only have a single estimation parameter, according to which the complex degree may be reduced effectively. The combined observation function is used to express the battery characteristics:

$$V = K_0 - RI - K_1/\Phi - K_2\Phi + K_3\ln(\Phi) + K_4\ln(1-\Phi) \tag{13}$$

where V is the battery terminal voltage; R is the battery IR and I is the current through it. $K_0 \sim K_4$ indicate the constant coefficient parameters. Ultimately, the SOC estimation model based on the EKF algorithm is constructed as shown:

$$\begin{cases} \Phi_{k+1} = \Phi_k + \frac{\Delta t \cdot \eta_1}{\eta_2 Q} I_k + \omega_k \\ V_k = K_0 - RI_k - K_1/\Phi_k - K_2\Phi_k + K_3 \ln(\Phi_k) \\ \quad + K_4 \ln(1-\Phi_k) + \nu_k \end{cases} \tag{14}$$

where η_1 is the Coulomb efficiency; η_2 is the revised coefficient of the battery terminal voltage; and Q indicates the calibrated battery capacity.

Real-time SOC estimation

Estimation process

The SOC, which acts in the similar role as the meter for the internal combustion engine system, is the most important factor for batteries that should be estimated accurately. In this paper, the initial value of the input parameters and the measurement current error may be corrected by using the proposed combined adaptive SOC estimation method, considering the parameters of temperature, charging current rate, discharging current rate, aging and so on. The estimation value is gradually close to the actual value detected by using the standard instrument and Ah integral method, reducing the accumulation error over time in the SOC estimation process.

The EKF method has performed well in the battery working state estimation, assuming the detection process noise is Gaussian white noise. However, the statistical and adaptive characteristics of the process noise are unknown when doing the actual BMS data acquisition in the working state monitoring process. The associated adaptive EKF method is introduced here, based on the EKF algorithm together with the Ah integral method and the OCV method. In the proposed estimation process, the state variables are estimated dynamically by using the measured data. Meanwhile, the statistical properties of noise are constantly estimated and revised. As a result, it may estimate the SOC value over time accurately for the LIB pack. According to Equations (1) and (2), the battery SOC estimation model may be obtained as shown in Equation (15). The state variables and output variables are represented by x and y, which are made by the appropriate variable matrix substitutions.

$$\begin{cases} x_{k+1} = A_k x_k + B_k u_k + \Gamma w_k, w_k(q_k, Q_k) \\ y_k = C_k x_k + D_k u_k + v_k, v_k(r_k, R_k) \end{cases} \tag{15}$$

where Γ is the interference matrix; w_k is the process noise, the mean value of which is represented by q_k and the covariance of which is characterized by Q_k. v_k is the measurement noise, and its mean value is characterized by r_k and its covariance value is characterized by R_k. Q_k, q_k, R_k and r_k are unknown, which are forecasted and estimated by using the EKF method. An adaptive EKF method for the SOC estimation is shown in Equations (16)–(20).

1) The initial estimation state factor x_{0_e} and its error covariance P_0 are set as the initial value obtained by using the mean and variance operation, respectively, which are described as:

$$\begin{cases} x_{0\_e} = E[x_0] \\ P_0 = E\left[(x_0 - x_{0\_e})(x_0 - x_{0\_e})^T\right] \end{cases} \tag{16}$$

2) The time point k status and its error covariance matrix could be updated by using the $k-1$ time point status and error covariance matrix together with the time point k input matrix, the process of which is:

$$\begin{cases} x_{k|k-1\_e} = A_k x_{k-1\_e} + B_k u_k + \Gamma q_{k-1} \\ P_{k|k-1} = A_k P_{k-1} A_k^T + \Gamma Q_{k-1} \Gamma^T \end{cases} \tag{17}$$

3) The Kalman gain matrix L_k may be determined by Equation (18), which should be used in the later time point k compound operation.

$$L_k = P_{k|k-1} C_k^T \left(C_k P_{k|k-1} C_k^T + R_{k-1}\right)^{-1} \tag{18}$$

4) The state equation and the observation equation should be used in the time point k state updating process, considering the estimation value and the measurement value at time point k. The status and state covariance matrix at time point k should be updated by using the time point k output error:

$$\begin{cases} x_{k\_e} = x_{k|k-1\_e} + L_k y_{k\_error} \\ P_k = (I - L_k C_k) P_{k|k-1} \\ y_{k\_error} = y_k - C_k x_{k|k-1} - D_k u_k - r_{k-1} \end{cases} \tag{19}$$

5) The mean and covariance value of the process noise together with the measurement noise should be updated according to:

$$\begin{cases} q_k = (1-d_{k-1}) q_{k-1} + d_{k-1} G \\ \quad (x_{k\_e} - A_k x_{k-1\_e} - B_k u_{k-1}) \\ Q_k = (1-d_{k-1}) Q_{k-1} + d_{k-1} G \\ \quad \left(L_k y_{k\_error} y_{k\_error}^T L_k^T + P_k - A_k P_{k|k-1} A_k^T\right) G^T \\ r_k = (1-d_{k-1}) r_{k-1} + d_{k-1} \\ \quad \left(y_k - C_k x_{k|k-1\_e} - D_k u_k\right) \\ R_k = (1-d_{k-1}) R_{k-1} + d_{k-1} \\ \quad \left(y_{k\_error} y_{k\_error}^T - C_k P_{k|k-1} C_k^T\right) \end{cases} \tag{20}$$

There are some parameters should be explained in the formula above. Γ is initiated as $\Gamma = diag(0.001\ 0.001\ 0.001)$; b is the forgetting factor and its range is $0 < b < 1$, which is set as $b = 0.98$ in this work. In order to improve the efficiency of program execution and shorten the execution time, the forgetting factor b is used to describe the aging characteristics of the power LIB in the paper, which has influence on the Coulomb efficiency calculation. The small value of the forgetting factor illustrates that the LIB has been used for a considerable time, which will make the remaining capacity low. Meanwhile, the large value of the forgetting factor illustrates that the LIB has been used for a short time, which will make the remaining capacity high. G is set as $G = (\Gamma^T \Gamma)^{-1} \Gamma^T$; d_k is set as

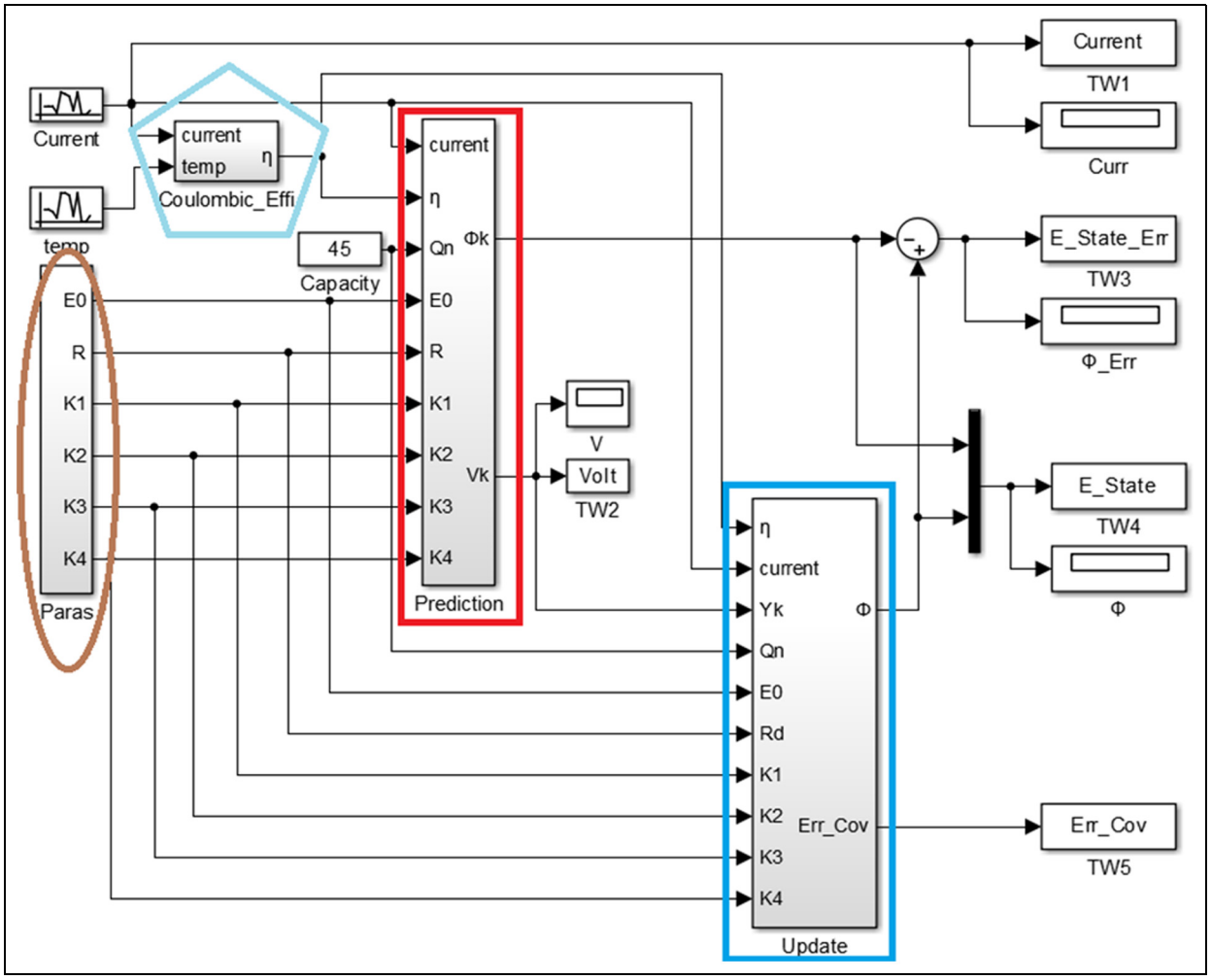

Figure 4. Over-all structure of the estimation model.

$d_k = (1 - b)/(1 - b^k)$. Thus, the state variable SOC may be constantly corrected by the online real-time estimation for q_k, r_k, Q_k and R_k, which improves the estimation accuracy correspondingly. As known from the SOC estimation process that is based on the improved EKF method, the combined adaptive SOC estimation method may perform the prediction and amendment during all the iterations, aiming to make the optimal estimation state value closer to the actual value and may realize the error correction effectively.

The overall structure of the estimation model is shown in Figure 4, in which the prediction and the update stage of the estimation process is signed and characterized by the red and blue rectangle. The battery model parameters are initially indicated using the input vector, which is marked with an oval. The input real-time data series including the current and temperature are started, and are handled by using the Coulombic efficiency process marked with the hexagon. This is gaining popularity in estimator design, as it achieves good simulation accuracy and is physically justifiable in providing limited insights into the electrochemical reactions to some extent, which has good performance in the working state estimation for the LIB pack.

Impact factor selection

As known from the LIB characteristic analysis, the battery capacity is mainly affected by charging current rate, discharging current rate, temperature, self-discharge and aging. From the self-correcting nature of the EKF algorithm, the battery self-discharge effect is not considered in the estimation process. Meanwhile, as the effects of battery aging may take quite a long time before they have any influence on the battery SOC estimation process, the effects of aging are not considered in the proposed method.

Charging and discharging current rate. The battery capacity is affected by the charging current rate and the discharging current rate enormously. When the maintenance current rate increases, the discharging electricity of the battery will be reduced. η_i is defined to express the current influence coefficient of the battery capacity, and therefore the actual capacity of the battery after the charging–discharging current rate correction is shown as:

$$Q_i = \eta_i Q_n \tag{21}$$

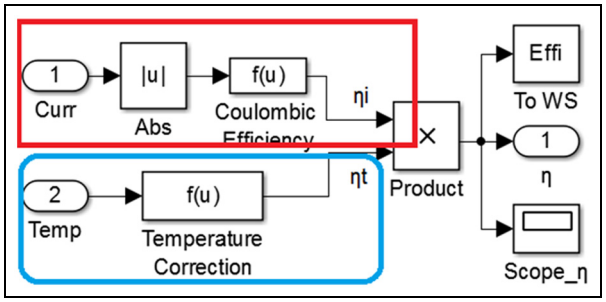

Figure 5. The impact factor influence correction sub-model.

where Q_i indicates the actual capacity of the battery for the discharging current i, and Q_n indicates the battery standard capacity. The different discharging rate experiments are done for the lithium iron phosphate battery cell at the room temperature (25°C), and the actual discharging capacity is calculated, in which the experimental data is obtained. The cftool toolbox in MATLAB is used to gain the curve of actual battery capacity and charging–discharging current rate. The second-order polynomial fitting factor of the battery actual capacity may be obtained by continuing to use the cftool toolbox as in:

$$\eta_i = (3.905i^2 - 123.6i + 15030)/14967 \tag{22}$$

where i indicates the discharging current and the realization of the influence parameter characterization is shown in Figure 5, which is indicated by the red rectangle. Its computational cost may be reduced by simply the model complexity with the benefit of physical insight, and has the best trade-off between the estimation accuracy and computational efficiency.

Temperature correction. The temperature influence on the battery capacity is also quite significant. When the temperature is low, the battery capacity will be reduced accordingly. η_T is defined as the temperature influence coefficient of the battery capacity, and the actual battery capacity after temperature correction is:

$$Q_T = \eta_T Q_n \tag{23}$$

where Q_T indicates the actual discharge capacity of the battery at time point T. In the condition of $SOC = 1$, the discharging capacity of LIB in the condition of standard charging–discharging current rate $C/30$ is obtained at various temperatures. The temperature influence coefficient of the fourth-order polynomial fitting for the actual battery capacity is:

$$\eta_T = -0.00000003637\mathrm{T}^4 + 0.000003521\mathrm{T}^3 - 0.0001373\mathrm{T}^2 + 0.006311\mathrm{T} + 0.8873 \tag{24}$$

where T indicates the actual working temperature of the battery, the unit of which is degree Celsius (°C). The influence function is realized in the impact factor influence sub-model, which is shown in Figure 5, the realization process of which is characterized by using the blue rectangle. Therefore, considering the effect of charging–discharging current rate and temperature, the actual battery capacity may be obtained by using the function $Q = \eta_i \eta_T Q_n$ and the total Coulomb efficiency may be characterized by using the function $\eta = \eta_i \eta_T$.

State-space model of the battery

As seen from the EKF algorithm analysis, the non-linear filtering problem of the discrete data may be solved recursively based on a series of mathematical formulas, which are able to estimate the process state by minimizing the state error covariance in the estimation process. In the estimation process, only the latest SOC value and its error covariance need to be known to obtain the current time state and its error covariance. There is no need to store large amounts of historical data, which makes the real-time characterization and estimation even better. Furthermore, concluding from the principle analysis, the EKF-based estimation algorithm has a self-correcting nature, which makes the filtering process exhibit no accumulated error, and therefore it has high accuracy. Thus, the proposed composite estimation algorithm is suitable for the SOC estimation of LIB.

Battery state equation. As seen from the standard non-linear state equation (shown in Equation 5), the state equation describes the state change law between two adjacent time points of the dynamic system. As the Ah integration method provides such a variety law, the battery state equation may be linearized by using the Ah integral method and the battery state equation not considering the process noise may be described as:

$$x_{k+1} = x_k - (\eta \Delta t / Q_n) I_{k+1} \tag{25}$$

As seen from the above equation, by introducing the Columbic efficiency parameter η and the interval time parameter Δt together with the rated capacity parameter Q_n, the SOC state value may be updated by using the current at time point $k + 1$ and the SOC state value at time point k. The state equation may be realized in the prediction sub-model of the estimation system shown in Figure 6, in which the blue box marked part is designed according to Equation (25).

The relationship of the parameters in the yellow oval marked part may be expressed as:

$$Fcn = u(1) * u(2) * u(4)/u(3) \tag{26}$$

As seen in the Figure 6 and compared with Equation (25), the parameters in Equation (26) have a direct corresponding relationship with the parameters in Equation (25), which may be described as:

$$\mathrm{u}(1) \to i_{k+1} \quad \mathrm{u}(2) \to \eta \quad \mathrm{u}(3) \to Q_n \quad \mathrm{u}(4) \to \Delta t \tag{27}$$

The state equation may be obtained accordingly by considering the process noise ω, which may be described as:

$$x_{k+1} = x_k - (\eta \Delta t / Q_n) I_{k+1} + \omega_{k+1} \tag{28}$$

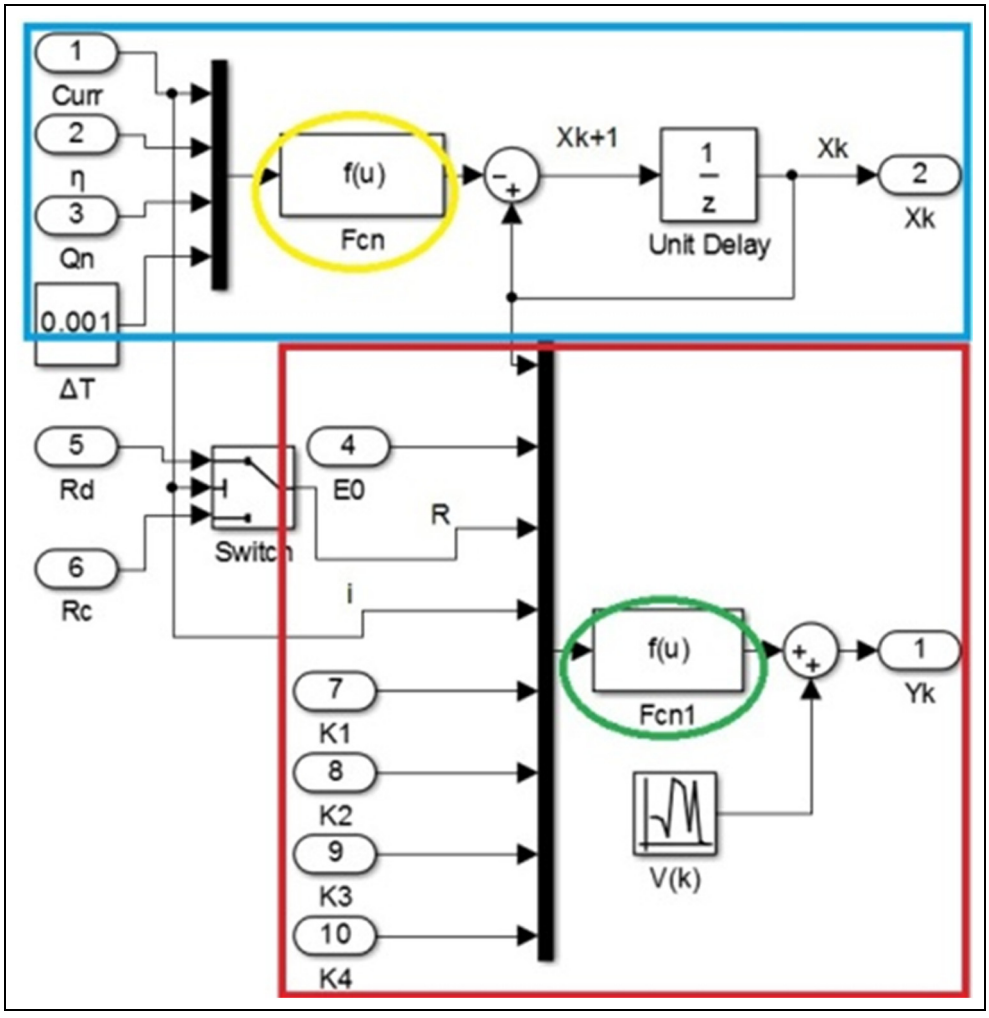

Figure 6. Prediction sub-model of the estimation process.

where x_k is the SOC value at the time point k; Δt is the discrete time interval; i_k is the discrete current; η is the Coulomb efficiency, which was described detail previously; and ω_k is the normal white noise with zero mean, the variance value of which may be expressed by using Q_n.

Battery measurement equation. The measurement equation describes the state of the observing signals. As seen from the OCV-based estimation method, the battery SOC value is relevant to its voltage value. As a result, the SOC observation may be realized by using this method. Many scholars have studied the electrochemical battery operated model to describe the battery output voltage. In order to improve the accuracy of the model, the model combined by Shepherd, Urmewehr universal and Nernst equations was proposed, the composition equation of which is shown in Equation (13), in which y_k is the battery terminal voltage; E_0 is the battery electromotive force when the initial battery SOC value is 1; and R is the IR, the value of which will change accordingly when the battery is in the discharging or charging working conditions.

The OCV is difficult to obtain, as it cannot be measured directly when the battery is in the charging or discharging process, so y_k is used instead of using the OCV approximately. At the same time, as the calculation amount of the composition model is quite small and the arithmetic operation is very simple, it is convenient to implement in the SCM. The combination model is used in the battery measurement equation. The measurement equation considering the measurement noise is shown in the second part of Equation (14), where v_k is the normal white noise with zero mean and its variance is characterized by using R_k, which is independent with the process noise. K_1, K_2, K_3 and K_4 are used as the model constant variable parameters. The column vector Y is set as $Y = [y_1, y_2, \ldots, y_n]^{\mathrm{T}}$ and the matrix H is set as $H = [h_1, h_2, \ldots, h_n]^T$, the elements of which are initiated according to one order vector $h_j = [1, i_j, 1/x_j, x_j, \ln(x_j), \ln(1 - x_j)]^T$.
The combined vector for the constant parameters are set as $\theta = [E_0, R, K_1, K_2, K_3, K_4]^T$ and $N = [\mu_1, \mu_2, \ldots, \mu_n]^T$. As a result, the matrix pattern measurement equation may be obtained and expressed according to the function $Y = H\theta + N$. Therefore, θ may be obtained as

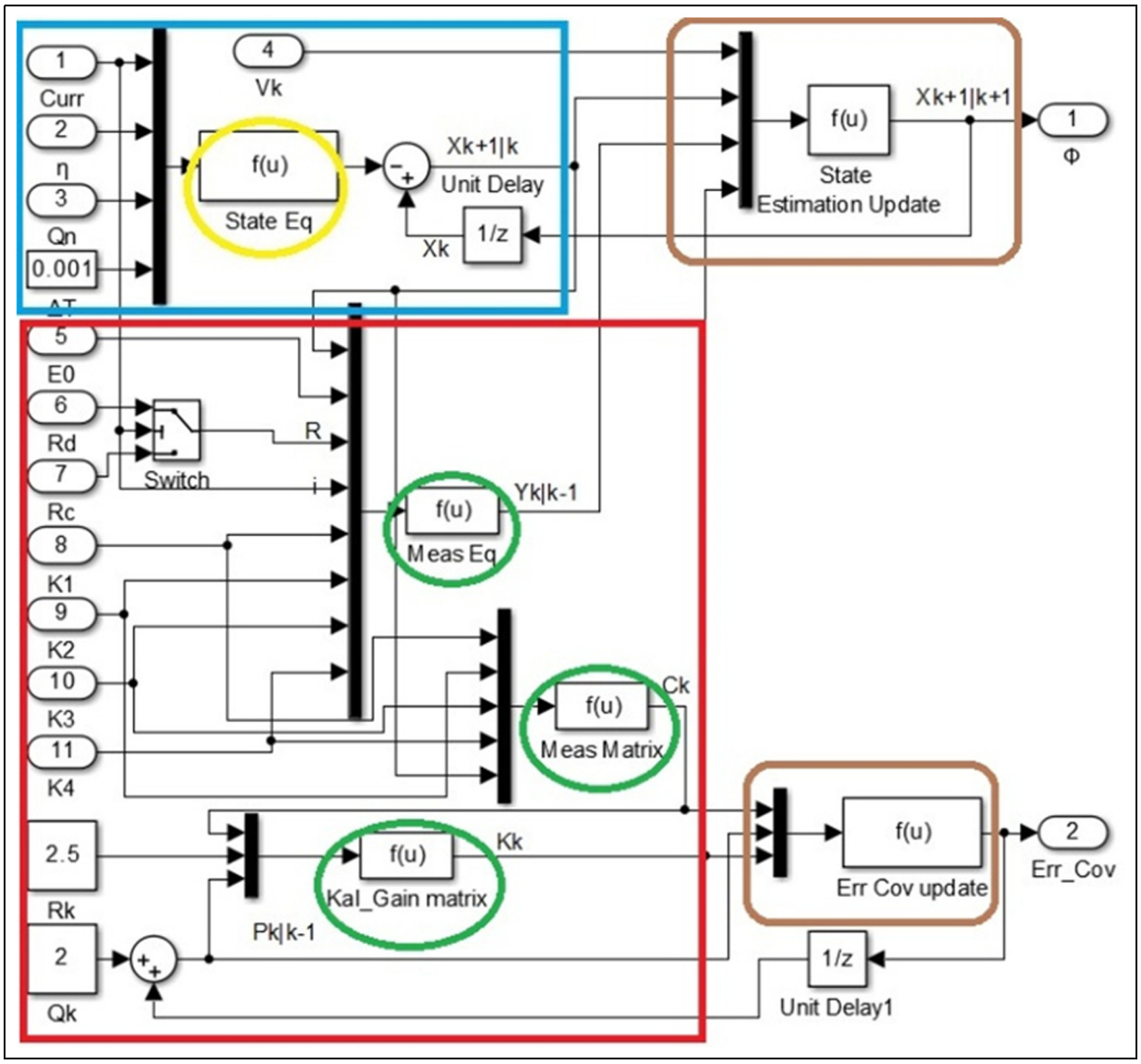

Figure 7. State update sub-model.

$\theta = (H^T H)^{-1} H^{-1} Y$. The measurement equation may be realized in the 'MeasEq' sub-model of the estimation system, which is shown in Figure 7, in which the red box marked part is designed according to the second part of Equation (14).

One way is to record the latest memorable battery state value immediately when the battery stops working, which may be used as the initial SOC value for the next estimation process. This approach is relatively simple, but there is a downside. Even if it is not running, but as the sole energy provider, it is still used for the weak powered part of the power supply system, such as LED lights and communication networks that are still in working condition, which will make the initial value error for each estimation process be increased. Even this small current may be detected and used in estimating the new SOC value, and the battery self-discharge current is too small to be detected. As a result, the reducing SOC value caused by the self-discharge cannot be estimated by using this method. Then the error of the SOC initial value will be significant after a long period of non-use.

The main function part not considering the noise as seen in Equation (13) is shown in the blue ellipse marked part of the Figure and expressed by using the function 'Fcn1' that is shown in Equation (29), in which the relationship of the parameters may be expressed.

$$Fcn1 = u(2) - u(3) * u(4) - u(5)/u(1) - u(6) * u(1) + u(7) * \log(u(1)) + u(8) * \log(1 - u(1)) \quad (29)$$

As seen in the Figure and compared with Equation (28), the parameters in Equation (29) have a direct corresponding relationship with the parameters in Equation (13), which may be described thus:

$$\begin{aligned} &u(1) \to x_k \quad u(2) \to E_0 \quad u(3) \to R \quad u(4) \to i_k \\ &u(5) \to K_1 \quad u(6) \to K_2 \quad u(7) \to K_3 \quad u(8) \to K_4 \end{aligned} \tag{30}$$

The combined parameter values, which are characterized by using the vector parameter θ, may be obtained as shown in Equation (31). The OCV–SOC curves are obtained by performing the HPPC experiments, and then the discharging efficiency is measured under different temperatures and different discharging current rates. The state-space equation is set and used in the parameter input module for the SOC estimation process of the power LIB pack, the parameters of which are realized by the polynomial curve fitting method of the OCV–SOC data sequence.

$$\theta = [3.391, 0.0048, -0.000268, 0.1495, 0.111, -0.01955]^{\mathrm{T}} \tag{31}$$

Implementation of the SOC estimation

Initial estimation parameters

The parameter initial values may be obtained by comparing the state-space model of the SOC estimation to the standard model of the EKF algorithm, which are described as:

$$\begin{cases} \Phi_k = 1, B_k = -\frac{\Delta t}{\eta_i \eta_T Q_n}, u_k = i, \\ H_k = \left.\frac{\partial y_k}{\partial x_k}\right|_{x_k = x_{k|k-1}} = \frac{K_1}{\left(x_{x|k-1}\right)^2} - K_2 + \frac{K_3}{x_{k|k-1}} - \frac{K_4}{1-x_{k|k-1}} \end{cases} \tag{32}$$

As the EKF algorithm has self-correction characteristics, the SOC estimation has a low dependence on the initial values, which may be set arbitrarily. However, if the initial SOC value deviates from the true value largely, it will lead to the computation time increase for the SOC estimation process compared with the initial value that at the vicinity of the actual value. For example, if the SOC value has not converged to the actual value, it is easy to cause battery over-discharge. As a result, when the battery SOC value is very small and has reached the low SOC warning value, it may cause the detriment of the battery life, leading to serious accidents. It is significant to make the initial SOC value close to the actual value and there are generally two approaches for obtaining the initial SOC value.

Another method is to correct the SOC value of the battery by using the OCV–SOC curve when the battery stops working, which is a more accurate way of determining the initial value of SOC. Meanwhile, it needs quite a long time to be shelved to cause the lithium ions to be in a stable state, by which the accurate initial SOC may be obtained and used in the next estimation stage. For determining the initial value of the error variance parameter $P_{0|0}$ of SOC, there are a large number of experiments performed and the experimental results are analysed, the analysis result of which shows that its value is not critical and any $P_{0|0} \neq 0$ may cause convergence of the estimation process. For the condition $P_{0|0} = 0$, if the SOC initial value also equals 0, it may cause the filter not to converge, resulting in SOC always being equal to 0. However, in the real application of the LIBs, the system will prompt the charge signal when the SOC value falls below a certain value, such as 10% and so on. In particular, if the voltage is lower than the discharging cut-off voltage (3.0 V or so), it will disconnect the battery power supply circuit loop to stop the discharging process, so this extreme condition will not occur in the actual power supply applications. The proposed framework is implemented on the LIB successfully with simulation and testing experiments.

Coefficient and its adjustment

The filter coefficients mean of the measurement is characterized by R_k and the process noise variance is expressed by Q_k, the values of which will affect largely to the SOC estimation effect. R_k may be obtained by using the off-line battery voltage detection and the analysis of the measurement equipments, but the core parameter SOC is difficult to obtain. The reason is that we cannot obtain the battery SOC value directly by using the measurement equipment and as a result we cannot obtain its error variance value. However, we may obtain the Q_k value that may reflect the process error variance effectively by comparing with R_k or using other passions. If the values for R_k and Q_k are not adequate, we may also adjust them by comparing with other estimation methods, aiming to improve better accuracy of the SOC estimation.

The SOC estimation model is constructed and realized with an emphasis on the estimation fusion strategy. Firstly, the input signal is produced and given as the input of the basic measurement model that is based on the ECM, as shown in Equations (3) and (4). Then, the Coulombic efficiency is calculated by using the equations described previously, which is also taking the current and temperature as input parameters, and its output value is used in the measurement sub-model and KF estimation sub-model. The state equation and measurement equation that were shown earlier are used in both measurement sub-model and the KF estimation sub-model. As a result, E_0, R, K_1, K_2, K_3 and K_4 are initiated and used according to Equation (32). At last, the estimation process is realized by using the following two sub-models step by step.

The measurement sub-model is constructed according to Equations (25) and (31), which are the state and measurement equations, the sub-model of which is shown in Figure 4. As the measurement sub-model is based on the general state and measurement equations, it may reflect the battery characteristics of the discharging working conditions. However, although it has very high accuracy, it also has low adaptive performance because it is based on the Ah and OCV methods. As a result, it is used as a correct part to make the EKF estimation sub-model more accurate. The EKF estimation sub-model is realized according to the estimation process described previously. The SOC estimation error covariance is also provided and used step by step in the estimation process.

Experimental analysis

The model core performance for the input parameter, estimation effect, coefficient effect and the battery model parameter vector is analysed in this section, the results of which are compared with the existing SOC estimation methods.

Figure 8. The battery maintenance and testing system (BMTS) for the maintenance of lithium-ion battery (LIB) packs.

Model input parameters

The BMTS has been designed and realized for the aerial LIB pack experiments, as shown in Figure 8. There is one industrial personal computer (IPC) used to realize the control strategies and the human–machine interface (HMI) is used as the monitoring interface. The keyboard and mouse are used to input the parameters and allow human control. There are 14 digital power supplies used for the balancing charging together with two large power supplies from Taiwan. The two electronic loads are used to practise the discharging. The protect unit is designed and used for real-time protection in the DCM process.

The protection unit is designed and used in the BMTS, which is shown in Figure 9.

The performance parameters of the LIB cell sample used in this paper are described as follows. The rated voltage is 3.7 V and the rated capacity is 45 Ah. The resistance is less than 3 mΩ and the discharge cut-off voltage is 2.8 V. The charging cut-off voltage is 4.15 V and the nominal discharging current is 45 A, which is also named as 1 C. The battery adaptive SOC estimation process uses the current, temperature and voltage as input parameters. The battery working current uses the normal signal with the mathematical expectation value of 7 and the variance value of 1, which is used to make the substation electrician current situation analogue. The experimental results for its performance characteristics are obtained and shown in Figure 10.

The capacity degradation is also studied by Landi et al. (2015, Figure 2) and Zheng et al. (2015, Figure 6), the results of which have the same varying regulation, and wider capacity and current rates are studied here to gain a comprehensive performance test. It has the same change regulation with the experimental results obtained by Corno and Bhatt (2015, Figure 6), which also proves its accuracy. Generally, the battery parameters are changing slowly. Thus, the update rate of LIB battery parameters, including their identification algorithm, needs not be too fast. Two forms of battery parameter identification are performed in our experiments, in which the identification algorithm runs every 300 s or only once.

Accordingly, the battery parameters are updated every 300 s or only once. The regression algorithm is used to identify the battery parameters. Its amount of computations is moderately large, and it is difficult to obtain battery parameter in each run. Fortunately, considering the slow rate of change of the battery parameters, the real-time requirements of the parameter identification algorithm are not very high, so battery parameters are not updated in each run but only a few times in our experiments. The voltage characteristic in the cycling maintenance process is shown in Figure 11, which has the same varying regulation as the charge and discharge experimental results obtained by Li D et al. (2015, Figure 5) and Liu et al. (2016, Figure 2). The battery voltage graph shows tendency to flatten between 3.8 and 4.1 V during the charging stage and between 4.0 and 3.7 V during the discharging stage, the results of which may also been obtained by Monem et al. (2015, Figure 2).

Similarly, the battery temperature uses the normal signal simulation with mathematical expectation of 35 and variance of 1, which indicates that the battery temperature is about 35°C and is in line with the normal distribution. The battery

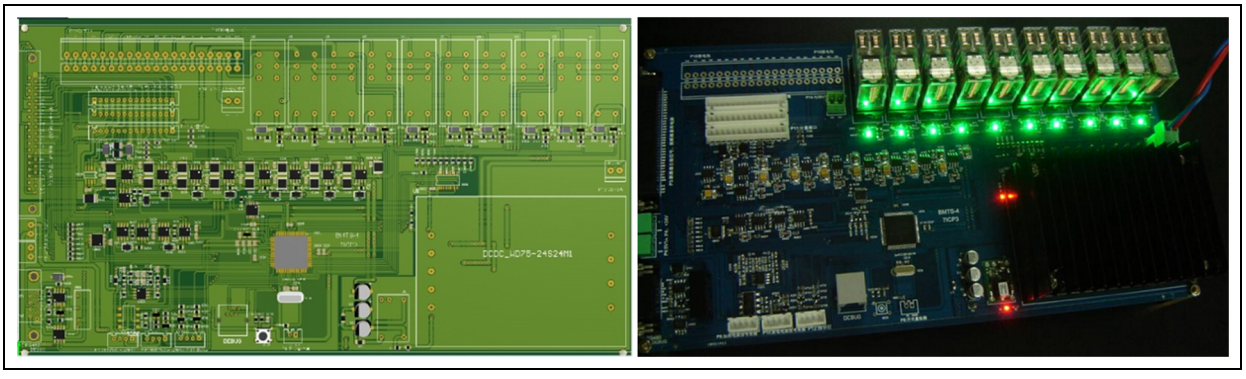

Figure 9. The protection unit designed for the battery maintenance and testing system (BMTS) of lithium-ion battery (LIB) packs.

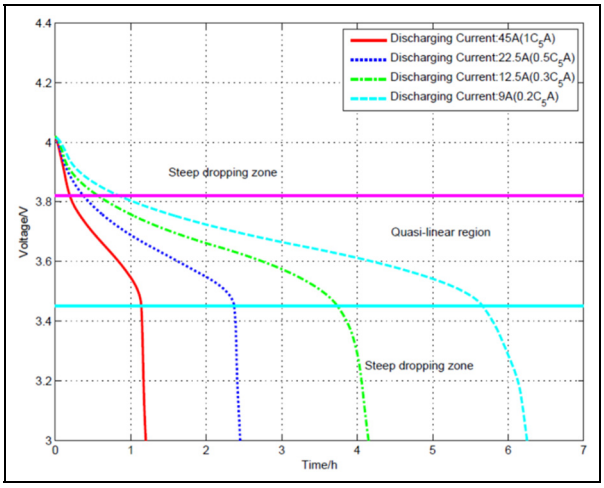

Figure 10. Different discharging current characteristics of power lithium-ion battery (LIB) cell.

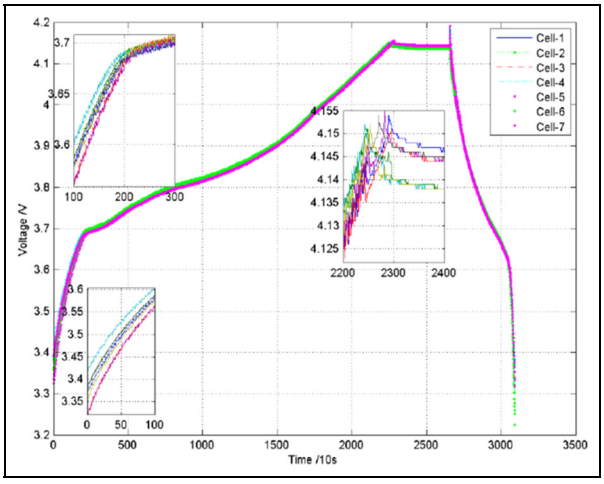

Figure 11. The voltage characteristics of the power lithium-ion battery (LIB) cells in the cycling maintenance process.

voltage is measured to obtain the initial SOC estimation value. As the cell voltage output of LIB is very stable, it may be measured by using accurate measuring equipment. The output voltage in the measurement equation is used to approximate the voltage measurement and a zero mean Gaussian measurement noise with the variance value of 0.00005 is then considered to obtain the discharging voltage curve.

Estimation effectiveness analysis

Considering the online SOC estimation demand by using the associated BMS equipment of the power LIB pack, the values of the measurement noise variance and the process noise variance are initiated. In order to match it, the values are also selected in simulation process. However, when doing the real-time SOC estimation process, the noise may vary along with the working time and the different values are studied in the experiments. The measurement noise variance may be set as $R_k = 2.5$ and process noise variance set as $Q_k = 2$. The initial error variance may be set as $P_{0|0} = 10$.

1) The estimation effect with large SOC initial value is analysed. When the SOC actual initial value is set as 0.8 and the initial SOC value of the filter is set as 1, the SOC estimation curve may be obtained as shown in the first part of Figure 8. The difference between the SOC estimation value and the actual SOC value of the LIB is about 0.2. However, the SOC value may converge to the actual value from the initial estimate value 1 quickly in the estimation process, fully reflecting the EKF self-tuning capabilities. Its absolute error curve may be obtained as shown in the second part of Figure 12.
As seen from Figure 10, the EKF has strong error correction capability for the SOC estimation process when the SOC initial value is large, the varying formula of which is similar with the experimental results obtained by Hua et al. (2015, Figure 6). The SOC estimation error becomes increasingly smaller along with

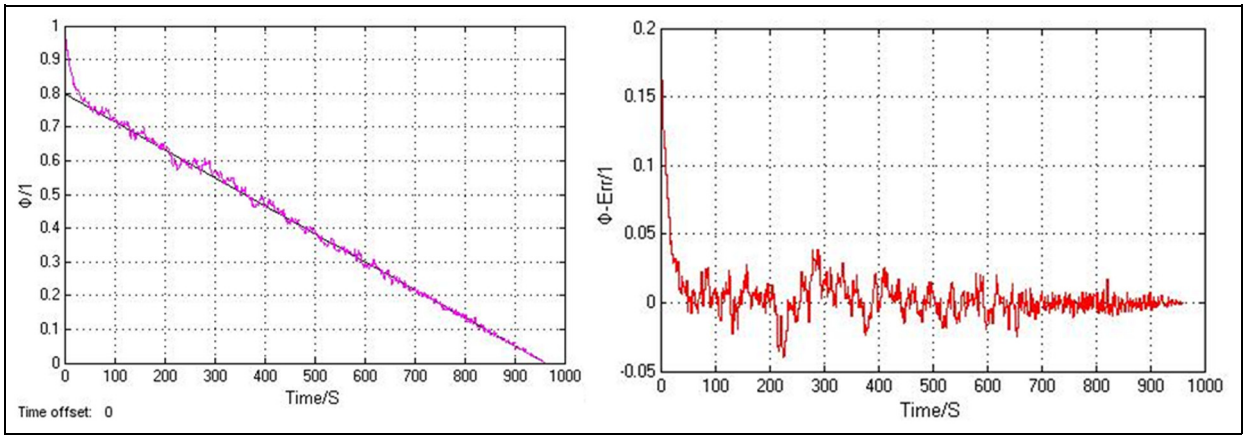

Figure 12. State of charge (SOC) estimation and its absolute error.

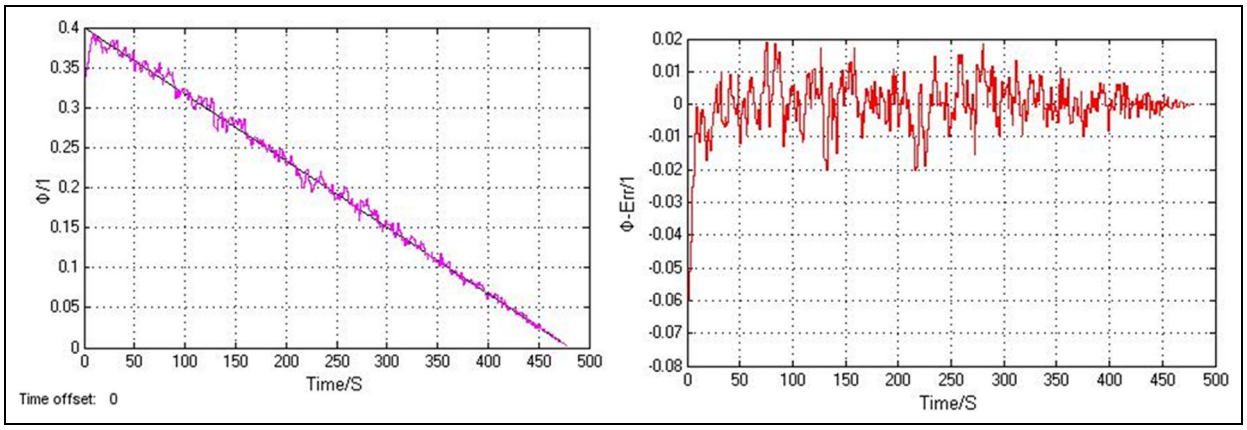

Figure 13. State of charge (SOC) estimation tracking effect and its absolute error.

the time spread, and its maximum absolute error is only 4.17% after the convergence, which also reflects its self-correcting capability and anti-jamming capability. Compared with the experimental results (absolute error 4.96%) obtained by Aung et al. (2016), it has much higher accuracy. However, in the early SOC estimation process, there is a certain amplitude jitter, which is due to the error between the SOC initial value, the actual value and the cell voltage measurement error. The easiest improvement in practice is that the SOC initial value of the cells may be set as statutory correction using the storied history information and the OCV. Then, the SOC initial value and the actual value may initially be very close, so that the initial SOC estimation value will converge faster and the error will be smaller, which makes the estimation effect more outstanding.

If the cell voltage measurement equipment with higher accuracy may be used, it will further reflect the correction role of EKF and greatly enhance the SOC estimation, which makes the convergence speed higher and reduces jitter in the initial SOC estimation. However, as we know, the relative change between the OCV and SOC is very small in the LIB charging and discharging platform. As a result, it is very difficult to improve the voltage measurement accuracy, which will also increase the hardware cost. It is necessary to do the trade-offs according to the SOC estimation accuracy. The other ways should be considered first in practice to improve the filter performance and SOC estimation effects.

2) The estimation effect with small SOC initial value is analysed. The actual SOC initial value is set as 0.4 and the initial SOC estimation value is set as 0.3. The estimation effect for the SOC estimation may be obtained as shown in the first part of Figure 13 and its absolute error may be obtained as shown in the second part of the figure, which has the same regulation studied by Xian et al (2014, figure 6).

When the filter SOC initial value is small and closer to the actual SOC value, the EKF convergence speed is very fast, as seen in Figure 9. In this case, the SOC estimation has high estimate accuracy and the maximum absolute error is only 1.83%, which has higher accuracy compared with the experimental results obtained by Hua et al. (2015, figures 7 and 16). Although the SOC estimation curve still shows some jitter sometimes, the error is very small and the impact is not great. As in the above analysis, the actual initial value will be corrected so that jitter is negligible. As seen from the simulation analysis, the lower the actual initial SOC value, the smaller the absolute estimation error and the better the estimation result. As seen from the analysis of simulation results, the combined adaptive battery SOC estimation method may realize the power battery SOC estimation with higher accuracy and timeliness. As seen by doing careful analysis, it is suitable for the state estimation of non-linear systems and has good estimation results. As the KF obtains an optimal value itself based on the minimum variance, the EKF used for the non-linear system just obtains a suboptimal estimation value.

Therefore, the estimation accuracy is determined by the state-space model of the system. Generally, the state equation that describes the state changes may be obtained easily, but the measurement equation for the state correction of the prior estimation is not easy to obtain. If the measurement equation is non-linear and the system linearization error is too large, it will lead to the reduction of the estimation accuracy, or even make the filter unable to work. As a result, for the battery system, the most important thing for the estimation process is to establish an accurate estimation practical battery dynamic model to obtain a more accurate measurement equation, thereby improving the SOC estimation results. As the EKF itself has the chattering phenomena, the solution is to develop different SOC estimation methods for different battery charging and discharging phase of the battery OCV–SOC curve. The cycle revolution of the combined adaptive estimation algorithm is 5 s, the first 4 s of which is used for the Ah calculation and the last 1 s is used for EKF correction, aiming to eliminate the accumulated error generation in the Ah integration process. The integration method not only decreases the estimation jitter but also reduces the computational load effectively.

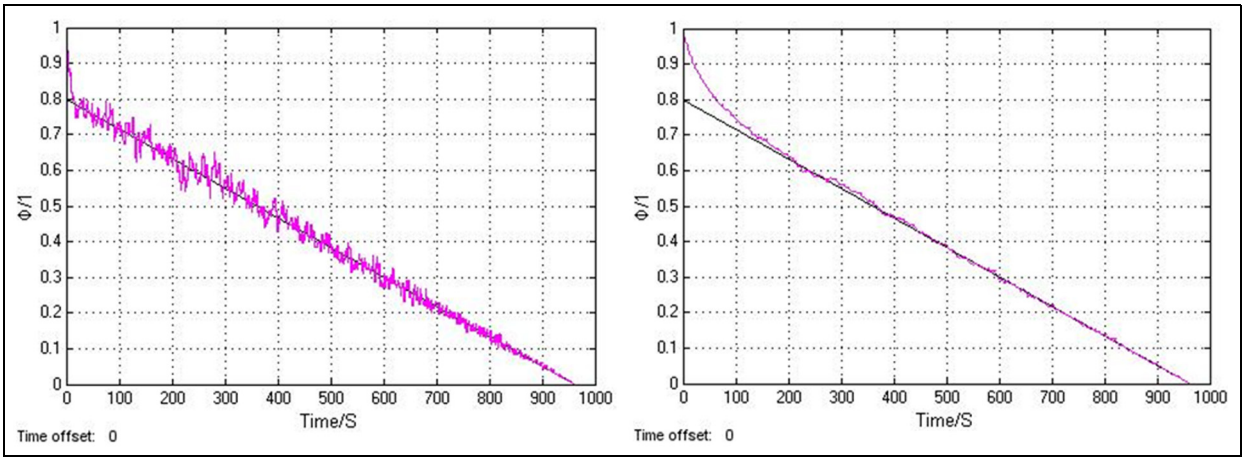

Figure 14. The state of charge (SOC) estimation when the variance changes.

Coefficient effect to the estimation

The estimation effect is obtained when the initial value is 0.8, the SOC initial value is 1, $R_k = 2.5$ and $Q_k = 2$, shown earlier. The following estimation effect analysis is done for the process noise variance increased by 10 times and reduced by 10 times.

When the variance parameter Q_k is set as 20, the estimation effect is obtained and shown in the first part of Figure 14. As seen from Figure 14, when the process noise variance is increased 10 times, it will result in the error variance increase of the SOC estimation together with the estimation absolute error increase. The estimation results obtained by Wang YZ et al. (2015, Figure 1) have the same varying regulation. There is a substantial jitter curve in the initial SOC estimation process at this time, in which the absolute maximum error convergence reaches 8.72%, but the filter converges to the theoretical value much faster. At this time, this is equivalent to reducing the measurement noise and the filter is more sensitive to the measurement voltage value, which leads to even faster convergence rate but makes the estimation jitter more serious. In addition, as seen from the Kalman gain calculation equation shown in Equation (27), the SOC estimation effect is the same whether the process noise variance is expanded 10 times or the measurement noise variance reduced 10 times.

When the variance parameter Q_k is set as 0.2, the estimation effect is obtained and shown in the second part of Figure 14. When the process noise variance is reduced 10 times, the SOC estimation error variance is reduced and the estimation absolute error is greatly reduced. At this time, the absolute maximum error is only 1.92% and the SOC estimation curve is very smooth, reflecting the characteristics of the estimation process with slow filtering convergence. The different initial SOC values, including 0.25, 0.4, 0.6, and 0.75 are analysed by Lee et al. (2015, Figure 13), showing high accuracy and adaptive advantages. This is almost equivalent to the measurement noise variance being increased10 times, compared with the estimation process described above. As seen from the above analysis, if the accuracy of the battery model or the cell voltage measurement is not high, a larger measurement noise variance or smaller process noise variance should be set to reduce the sensitive level of the estimation process to the voltage measurement value, so that the filter may be made much smoother, but this also reduces the estimation convergence rate, reducing the correction performance. It also illustrates the importance of battery modelling and the higher precision cell voltage measurement, as we have to ensure the hardware costs within an appropriate range. Therefore, the process noise variance or measurement noise variance should be adjusted in the simulation model, aiming to obtain a satisfactory result with the convergence rate and SOC estimation accuracy.

Battery model parameter vector effect

The battery is a complex electrochemical system, and the parameters of the battery model inevitably change in long-term application, that is as the battery ages. Battery aging will lead to the decreases of the battery actual total capacity and an increase in resistance, and the other model parameters will change as well; model parameter identification also has a certain error. Therefore, it is necessary to analyse the impacts of model parameters to evaluate their effect on the SOC estimation process.

When the battery is aging, the total capacity Q_n will be reduced, and the battery will be scrapped when the total battery capacity is reduced to 80% of the rated capacity, which may be seen in Figure 11. Meanwhile, as seen from the battery capacity characteristics, the battery actual total capacity is different with the working environment. Here, the total battery capacity is set as 95% of the rated capacity and the remaining settings are same as the results shown previously. In different OCV–SOC experiments, the obtained experimental results are slightly different and the identification parameters of the SOC estimation model are slightly changed. In considering this change, the adaptability of the parameter variation in the SOC estimation process needs to be verified. The simulation experiments are done when the combined model parameters have little change compared with Equation (31) and the parameter vector values are shown as:

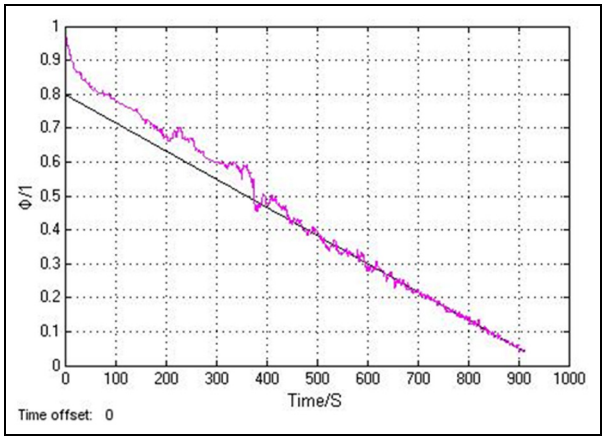

Figure 15. The state of charge (SOC) estimation with model parameter changes.

$$\theta = [3.391,\ 0.0048,\ -0.000368,\ 0.2525,\ 0.119,\ -0.02285]^{\mathrm{T}} \quad (33)$$

The SOC estimation results are shown in Figure 15. In this case, the estimation speed for the SOC convergence becomes slower, and there are substantial jitters in the initial SOC estimation process. The estimation absolute maximum error is 5.17% and the estimation effect changes violently. The performance degradation is up to 23.98% and the absolute maximum error is 4.17% in the correct parameter identification process.

As seen from the experimental results, the estimation effect is almost the same, and the maximum absolute error is 4.18%, which is just a small change compared with the maximum absolute error 4.17% of the rated capacity. It has similar regulation with the experimental results obtained by Hussein et al. (2016, Figures 4 and 5) and better astringency than the experimental results obtained by Olivares et al. (2013, Figure 6). Thus, the proposed SOC estimation method has good performance for the battery capacity decrease due to aging and incorrect identification of the battery total capacity.

When the battery is aging, the battery IR parameter R will increase, and the battery IR identification may not be correct. Here, the resistance increases only twofold, and the SOC simulation analysis result is that the maximum absolute error is 4.19%, which is little change compared with the maximum absolute error 4.17% in the correct parameter identification. As a result, the SOC estimation method has good performance when the resistance increases caused by aging resistance or its identification is not correct. When the identification for the OCV E_0 is incorrect and the OCV is set as 90% of the correct identification value, the SOC estimation maximum absolute error is 4.19% obtained by the simulation analysis, which is a small change compared with the maximum absolute error 4.17% by identifying the correct OCV value. As a result, the SOC estimation method still has a good estimate performance of the OCV when the battery fully charged and the identification is incorrect.

To sum up, the model estimation results change little when there is a slight parameter change in the proposed SOC estimation process of LIBs. Relative to the total battery capacity, IR, OCV of full charge, the combined model parameters K_1, K_2, K_3 and K_4 have greater effects on SOC estimation. As seen in the above experiment results, the combined SOC estimation model mainly based on EKF is quite effective, which is combined with the Ah and OCV methods. The measurement equation used in the estimation model is based on the composition equation of Shepherd model, Urmewehr universal model and Nernst model, which has good performance in the estimation process. The higher efficiency makes the proposed methodology more suitable for onboard estimation devices that require computationally efficient estimation techniques. Thus, it is of significant importance to extend the proposed framework from the cell level to the pack level in order to make it practically useful.

Conclusion

The SOC plays an essential role in many battery-powered applications and its adaptive estimation is of practical significance for the LIBs because of its time-varying performance and non-liner characteristics. In this paper, a high-power SOC adaptive estimation method was proposed, the main contents of which are shown as follows. The working properties of LIBs are analysed, including the cycle life characteristics, voltage characteristics and capacity characteristics. The comprehensive SOC estimation method was proposed and realized based on the battery core factors. The voltage characteristics of an LIB are highly non-linear and the SOC value is affected by the charging–discharging rate, temperature, aging, self-discharge and other factors. The main advantages of the proposed method are easy implementation, real-time performance and high accuracy. The establishment of the battery state-space model is constructed using discharging test data, the capacity influence coefficient, temperature coefficient and so on. The Ah method is used to obtain the state equation and the combination model to obtain the measurement equation. Then, the real-time correction of the total battery capacity is done to improve the estimation accuracy. The establishment of estimation model is done to analyse the SOC estimate effect, and the filter coefficients are given slight changes to evaluate the impact effect of the model parameters on the filtering performance. The experiment results show that this method has good SOC estimation results and the estimation process may be optimized by regulating the process noise variance, in which the model parameters varied slightly and have less impact on the filtering effect.

Declaration of conflicting interest

The authors declare that there is no conflict of interest.

Funding

The work was supported by the Sichuan Science and Technology Support Program (No. 2017FZ0013) and the Mianyang Science and Technology Project (No. 15G-03-3). Early work was supported by the Photoelectric Detection

National Defense Scientific Research (No. B3120133002) and the Special Environment Integrated Testing - Laboratory Robotics Project (No. 13zxtk0502). We would like to thank the sponsors.

References

Arbabzadeh M, Johnson JX and Keoleian GA (2016) Twelve principles for green energy storage in grid applications. *Environmental Science & Technology* 50(2): 1046–1055.

Aung H, Low KS and Goh ST (2015) State-of-charge estimation of lithium-ion battery using square root spherical unscented Kalman filter (Sqrt-UKFST) in nanosatellite. *IEEE Transactions on Power Electronics* 30(9): 4774–4783.

Beattie SD, Loveridge MJ and Lain MJ (2016) Understanding capacity fade in silicon based electrodes for lithium-ion batteries using three electrode cells and upper cut-off voltage studies. *Journal of Power Sources* 302: 426–430.

Burgos-Mellado C, Orchard ME and Kazerani M (2016) Particle-filtering-based estimation of maximum available power state in lithium-ion batteries. *Applied Energy* 161: 349–363.

Burow D, Sergeeva K and Calles S (2016) Inhomogeneous degradation of graphite anodes in automotive lithium ion batteries under low-temperature pulse cycling conditions. *Journal of Power Sources* 307: 806–814.

Cao Q and Zhong MY (2016) An adaptive strong tracking Kalman filter for position and orientation system. *Transactions of the Institute of Measurement and Control* 38(10): 1212–1224.

Ciez RE and Whitacre JF (2016) Comparative techno-economic analysis of hybrid micro-grid systems utilizing different battery types. *Energy Conversion and Management* 112: 435–444.

Corno M and Bhatt N (2015) Electrochemical model-based state of charge estimation for Li-ion cells. *IEEE Transactions on Control Systems Technology* 23(1): 117–127.

Dong GZ, Chen ZH and Wei JW (2016) An online model-based method for state of energy estimation of lithium-ion batteries using dual filters. *Journal of Power Sources* 301: 277–286.

Elsayed AT, Lashway CR and Mohammed OA (2016) Advanced battery management and diagnostic system for smart grid infrastructure. *IEEE Transactions on Smart Grid* 7(2): 897–905.

Fabri SG and Bugeja MK (2015) Functional adaptive dual control of a class of nonlinear MIMO systems. *Transactions of the Institute of Measurement and Control* 37(8): 1009–1025.

Fridholm B, Wik T and Nilsson M (2016) Robust recursive impedance estimation for automotive lithium-ion batteries. *Journal of Power Sources* 304: 33–41.

Gallien T, Krenn H and Fischer R (2015) Magnetism versus LiFePO4 battery's state of charge: a feasibility study for magnetic-based charge monitoring. *IEEE Transactions on Instrumentation and Measurement* 64(11): 2959–2964.

Ganesan N, Basu S and Hariharan KS (2016) Physics based modeling of a series parallel battery pack for asymmetry analysis, predictive control and life extension. *Journal of Power Sources* 322: 57–67.

Gao JP, Zhang YZ and He HW (2015) A real-time joint estimator for model parameters and state of charge of lithium-ion batteries in electric vehicles. *Energies* 8(8): 8594–8612.

Ge H, Huang J and Zhang JB (2016) Temperature-adaptive alternating current preheating of lithium-ion batteries with lithium deposition prevention. *Journal of the Electrochemical Society* 163(2): A290–A299.

He HW, Zhang YZ and Xiong R (2015) A novel Gaussian model based battery state estimation approach: state-of-energy. *Applied Energy* 151: 41–48.

Hua Y, Xu M and Li M (2015) Estimation of state of charge for two types of lithium-ion batteries by nonlinear predictive filter for electric vehicles. *Energies* 8(5): 3556–3577.

Hu YR and Wang YY (2015) Two time-scaled battery model identification with application to battery state estimation. *IEEE Transactions on Control Systems Technology* 23(3): 1180–1188.

Hua Y, Xu M and Li M (2015) Estimation of state of charge for two types of lithium-ion batteries by nonlinear predictive filter for electric vehicles. *Energies* 8(5): 3556–3576.

Hussein AA (2015) Capacity fade estimation in electric vehicle Li-ion batteries using artificial neural networks. *IEEE Transactions on Industry Applications* 51(3): 2321–2330.

Hussein AA, Fardoun AA and Stephen SS (2016) An online frequency tracking algorithm using terminal voltage spectroscopy for battery optimal charging. *IEEE Transactions on Sustainable Energy* 7(1): 32–40.

Jaguemont J, Boulon L and Dube Y (2016) A comprehensive review of lithium-ion batteries used in hybrid and electric vehicles at cold temperatures. *Applied Energy* 164: 99–114.

Jia B and Xin M (2015) Multiple sensor estimation using a new fifth-degree cubature information filter. *Transactions of the Institute of Measurement and Control* 37(1): 15–24.

Kim J (2016) Discrete wavelet transform-based feature extraction of experimental voltage signal for Li-ion cell consistency. *IEEE Transactions on Vehicular Technology* 65(3): 1150–1161.

Klein M, Tong S and Park JW (2016) In-plane nonuniform temperature effects on the performance of a large-format lithium-ion pouch cell. *Applied Energy* 165: 639–647.

Landi M and Gross G (2014) Measurement techniques for online battery state of health estimation in vehicle-to-grid applications. *IEEE Transactions on Instrumentation and Measurement* 63(5): 1224–1234.

Lee S, Kim J and Cho BH (2015) Maximum pulse current estimation for high accuracy power capability prediction of a Li-ion battery. *Microelectronics Reliability* 55(3): 572–581.

Li D, Ouyang J and Li HQ (2015) State of charge estimation for LiMn2O4 power battery based on strong tracking sigma point Kalman filter. *Journal of Power Sources* 279: 439–449.

Li Y, Zhang K and Zheng BL (2016) Effect of local deformation on the coupling between diffusion and stress in lithium-ion battery. *International Journal of Solids and Structures* 87: 81–89.

Lim K, Bastawrous HA and Duong VH (2016) Fading Kalman filter-based real-time state of charge estimation in LiFePO4 battery-powered electric vehicles. *Applied Energy* 169: 40–48.

Liu CF, Neale ZG and Cao GZ (2016) Understanding electrochemical potentials of cathode materials in rechargeable batteries. *Materials Today* 19(2): 109–123.

Lu B, Song YC and Zhang JQ (2016) Selection of charge methods for lithium ion batteries by considering diffusion induced stress and charge time. *Journal of Power Sources* 320: 104–110.

Masoumnezhad M, Jamali A and Nariman-zadeh N (2015) Optimal design of symmetrical/asymmetrical sigma-point Kalman filter using genetic algorithms. *Transactions of the Institute of Measurement and Control* 37(3): 425–432.

Masoumnezhad M, Jamali A and Nariman-zadeh N (2016) Robust GMDH-type neural network with unscented Kalman filter for non-linear systems. *Transactions of the Institute of Measurement and Control* 38(8): 992–1003.

Mohammad MA and Mohammad H (2016) Robust estimation of arc length in a GMAW process by an adaptive extended Kalman filter. *Transactions of the Institute of Measurement and Control* 38(11): 1334–1344.

Monem MA, Trad K and Omar N (2015) Lithium-ion batteries: evaluation study of different charging methodologies based on aging process. *Applied Energy* 152: 143–155.

Olivares BE, Munoz MAC and Orchard ME (2013) Particle-filtering-based prognosis framework for energy storage devices with a statistical characterization of state-of-health regeneration phenomena. *IEEE Transactions on Instrumentation and Measurement* 62(2): 364–376.

Panchal S, Dincer I and Agelin-Chaab M (2016) Experimental and theoretical investigation of temperature distributions in a prismatic lithium-ion battery. *International Journal of Thermal Sciences* 99: 204–212.

Perez G, Garmendia M and Reynaud JF (2015) Enhanced closed loop state of charge estimator for lithium-ion batteries based on extended Kalman filter. *Applied Energy* 155: 834–845.

Pramanik S and Anwar S (2016) Electrochemical model based charge optimization for lithium-ion batteries. *Journal of Power Sources* 313: 164–177.

Rahman MA, Anwar S and Izadian A (2016) Electrochemical model parameter identification of a lithium-ion battery using particle swarm optimization method. *Journal of Power Sources* 307: 86–97.

Raisemche A, Boukhnifer M and Diallo D (2016) New fault-tolerant control architectures based on voting algorithms for electric vehicle induction motor drive. *Transactions of the Institute of Measurement and Control* 38(9): 1120–1135.

Samadani E, Mastali M and Farhad S (2016) Li-ion battery performance and degradation in electric vehicles under different usage scenarios. *International Journal of Energy Research* 40(3): 379–392.

Saw LH, Ye YH and Tay AAO (2016) Integration issues of lithium-ion battery into electric vehicles battery pack. *Journal of Cleaner Production* 113: 1032–1045.

Schindler S, Bauer M and Petzl M (2016) Voltage relaxation and impedance spectroscopy as in-operando methods for the detection of lithium plating on graphitic anodes in commercial lithium-ion cells. *Journal of Power Sources* 304: 170–180.

Shang LP, Wang SL and Li ZF (2014) A novel lithium-ion battery balancing strategy based on global best-first and integrated imbalance calculation. *International Journal of Electrochemical Science* 9(11): 6213–6224.

Sidhu A, Izadian A and Anwar S (2015) Adaptive nonlinear model-based fault diagnosis of Li-ion batteries. *IEEE Transactions on Industrial Electronics* 62(2): 1002–1011.

Song ZY, Hofmann H and Li JQ (2015) Optimization for a hybrid energy storage system in electric vehicles using dynamic programming approach. *Applied Energy* 139: 151–162.

Su LS, Zhang JB and Wang CJ (2016) Identifying main factors of capacity fading in lithium ion cells using orthogonal design of experiments. *Applied Energy* 163: 201–210.

Tabuchi M, Kageyama H and Kubota K (2016) Structural change during charge-discharge for iron substituted lithium manganese oxide. *Journal of Power Sources* 318: 18–25.

Tenfen D, Finardi EC and Delinchant B (2016) Lithium-ion battery modelling for the energy management problem of microgrids. *IET Generation Transmission & Distribution* 10(3): 576–584.

Tong SJ, Klein MP and Park JW (2015) On-line optimization of battery open circuit voltage for improved state-of-charge and state-of-health estimation. *Journal of Power Sources* 293: 416–428.

Wang LM, Cheng Y and Zhao XL (2015) A LiFePO4 battery pack capacity estimation approach considering in-parallel cell safety in electric vehicles. *Applied Energy* 142: 293–302.

Wang QS, Sun QJ and Ping P (2016) Heat transfer in the dynamic cycling of lithium-titanate batteries. *International Journal of Heat and Mass Transfer* 93: 896–905.

Wang SL, Shang LP and Li ZF (2015) Lithium-ion battery security guaranteeing method study based on the state of charge estimation. *International Journal of Electrochemical Science* 10(6): 5130–5151.

Wang SL, Shang LP and Li ZF (2016) Online dynamic equalization adjustment of high-power lithium-ion battery packs based on the state of balance estimation. *Applied Energy* 166: 44–58.

Wang YZ and Hu HJ (2015) Pseudo distributed optimal state estimation for a class of networked systems. *Transactions of the Institute of Measurement and Control* 37(10): 1232–1241.

Wijewardana S, Vepa R and Shaheed MH (2016) Dynamic battery cell model and state of charge estimation. *Journal of Power Sources* 308: 109–120.

Xian WM, Long B and Li M (2014) Prognostics of lithium-ion batteries based on the verhulst model, particle swarm optimization and particle filter. *IEEE Transactions on Instrumentation and Measurement* 63(1): 2–17.

Yang WA, Xiao MH and Zhou W (2016) A hybrid prognostic approach for remaining useful life prediction of lithium-ion batteries. *Shock and Vibration* 2016: 1–15.

Ye YH, Shi YX and Saw LH (2016) Performance assessment and optimization of a heat pipe thermal management system for fast charging lithium ion battery packs. *International Journal of Heat and Mass Transfer* 92: 893–903.

Yu JB (2015) State-of-health monitoring and prediction of lithium-ion battery using probabilistic indication and state-space model. *IEEE Transactions on Instrumentation and Measurement* 64(11): 2937–2949.

Zhai SD and Yang XS (2014) Controllability of a class of switching control systems and application to the Kinetic Battery Model. *Transactions of the Institute of Measurement and Control* 4: 559–564.

Zheng YJ, Ouyang MG and Lu LG (2015) Study on the correlation between state of charge and Coulombic efficiency for commercial lithium ion batteries. *Journal of Power Sources* 289: 81–90.

Zhu JG, Sun ZC and Wei XZ (2016) Studies on the medium-frequency impedance arc for Lithium-ion batteries considering various alternating current amplitudes. *Journal of Applied Electrochemistry* 46(2): 157–167.